Supplementary Information: Hierarchical composition of reliable recombinase logic devices.

Sarah Guiziou[1], Pauline Mayonove[1], and Jerome Bonnet*[1]

[1]Centre de Biochimie Structurale, INSERM U1054, CNRS UMR5048, University of Montpellier, France.

*To whom correspondence should be addressed: jerome.bonnet@inserm.fr

These supplementary materials contain:

-Supplementary Figures S1 to S9.

-Supplementary Tables S1.

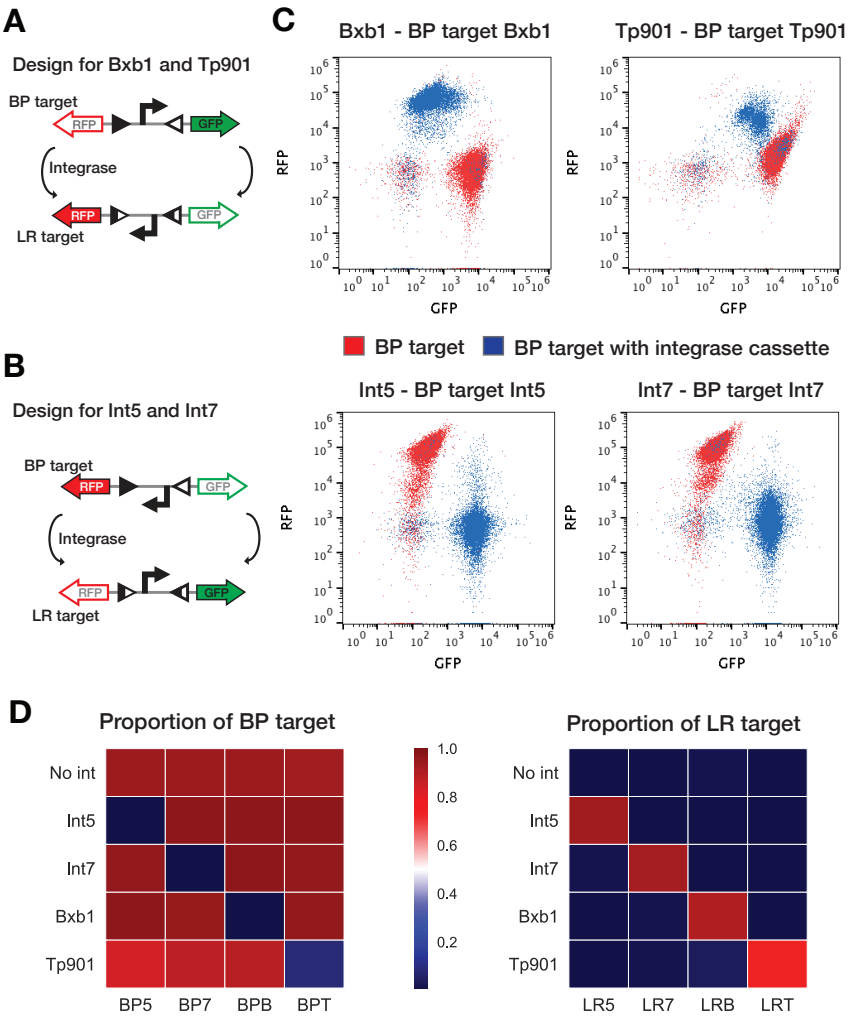

Figure S1: **Characterization and orthogonality of 4 serine integrases used in this study.** (A) and (B): Design of BP targets for the integrases. (A) For Bxb1 and Tp901 integrase, in presence of the integrase, gene expression switches from GFP to RFP via promoter inversion (B) for Int5 and Int7, gene expression switches from RFP to GFP. (C) Characterization of each integrase via co-transformation with BP targets. The graphs correspond to the density plots of flow-cytometer experiments with GFP over RFP fluorescence intensity in arbitrary unit. The red dots are *E. coli* strains with BP targets and the blue dots are *E. coli* co-transformed with BP targets and corresponding integrase cassettes. Cells are grown overnight in LB, and with the corresponding inducers for the expression of integrases. (D) Heatmaps of the proportion of BP target (left side) and LR target (right side) in the population of bacteria measured by flow-cytometer. For both heatmaps, each square corresponds to a co-transformation of one integrase cassette or none (labeled in y axis) with one BP target (labeled in x axis, BP5 for Int5, BP7 for Int7, BPB for Bxb1 integrase and BPT for Tp901 integrase).

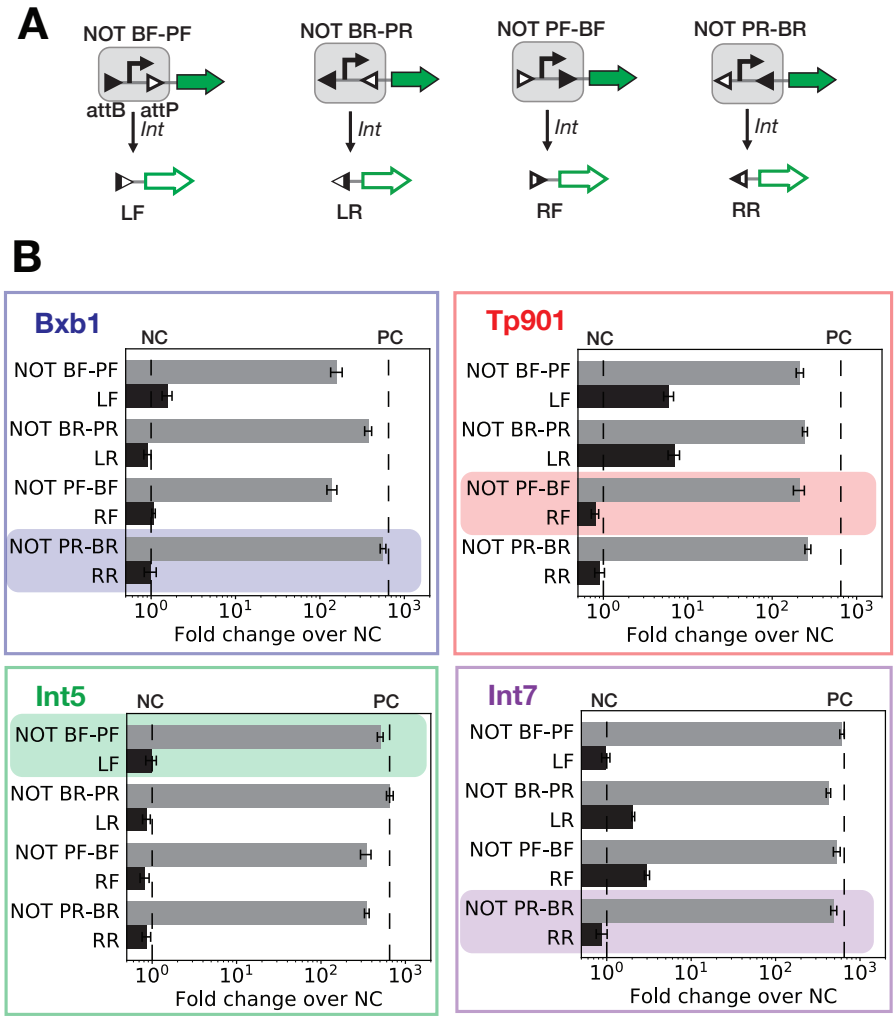

Figure S2: **Detailed histograms of NOT elements characterization.** (A) The 4 possible designs for NOT-elements, with a promoter flanked by integrase sites, and the corresponding constructs after excision mediated by the integrase. Triangles correspond to the integrase sites, attB site in black, attP site in white and attL or attR in black and white. F denotes sites in forward orientation and R for reverse. The gene coding sequence is a superfolder GFP and the promoter is the P7 promoter. (B) Bar graphs correspond to the fold change in mean fluorescence intensity of constructs compared to the negative control. Data were obtained by flow-cytometry measurement using 3 replicates per experiments, from 3 experiments performed on different days. The grey bars correspond to NOT-elements and the black bars for the attL and attR sites resulting from integrase-mediated excision. The dash lines correspond to fold change of the negative control (NC, equal to 1) and the fold change of the positive control (construct with only promoter P7). Error bars represent the standard deviation between the three experiments.The bars surrounded by a colored box correspond to elements that were selected for assembling recombinase logic devices.

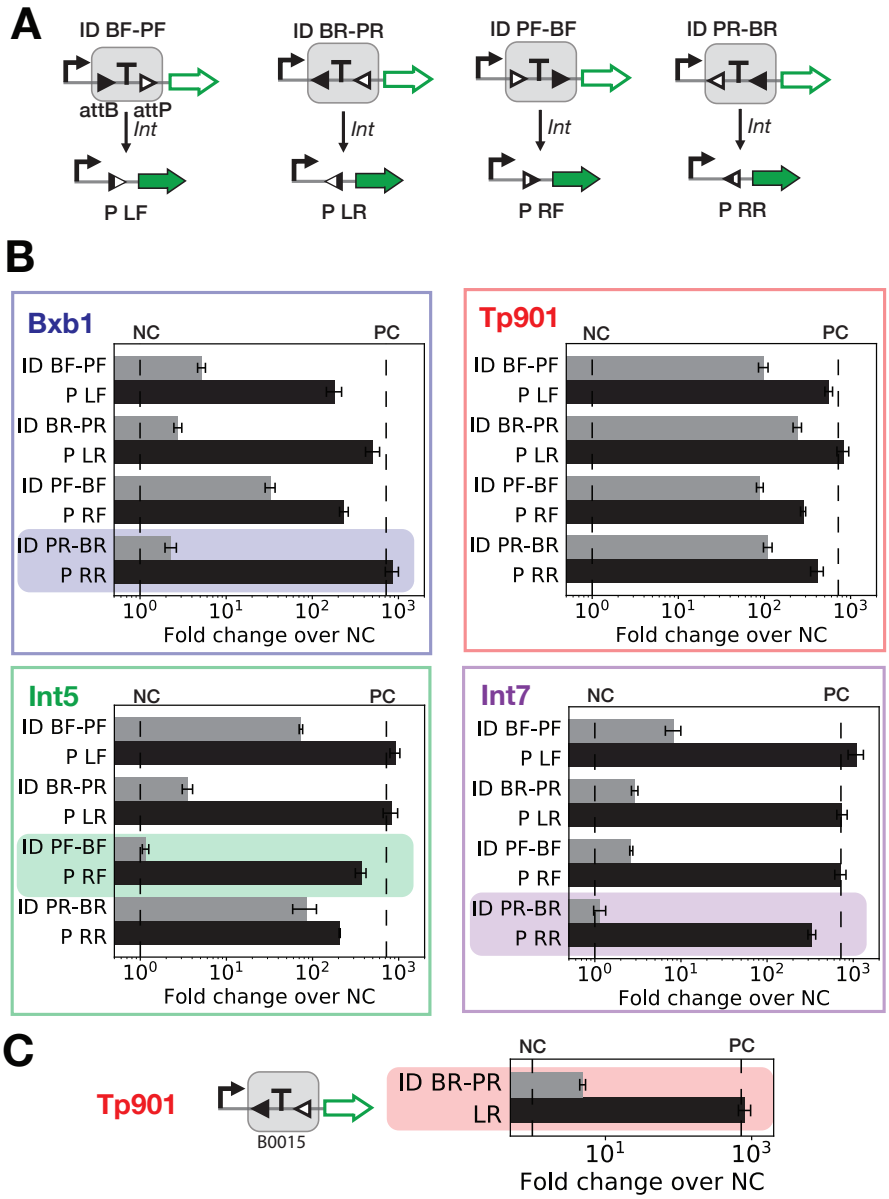

Figure S3: **Detailed histograms of ID elements characterization.** (A) The 4 possible designs for ID-elements with a terminator flanked by an integrase site pair, and the corresponding constructs after integrase-mediated excision. The gene coding sequence is a superfolder GFP and the promoter, the P7 promoter. (B) and (C) Bar graphs correspond to the fold change of mean of fluorescence intensity compared to the negative control. Data were obtained by flow-cytometry measurement with 3 replicates per experiments, from 3 experiments performed on different days. The grey bars correspond to ID-elements and the black bars for the attL and attR sites resulting from integrase-mediated excision. The dash lines correspond to fold change of the negative control (NC, equal to 1) and the fold change of the positive control (construct with only promoter P7: 650). Error bars represent the standard deviation between the three experiments. The bars surrounded by a colored box correspond to elements that were selected for assembling recombinase logic devices.

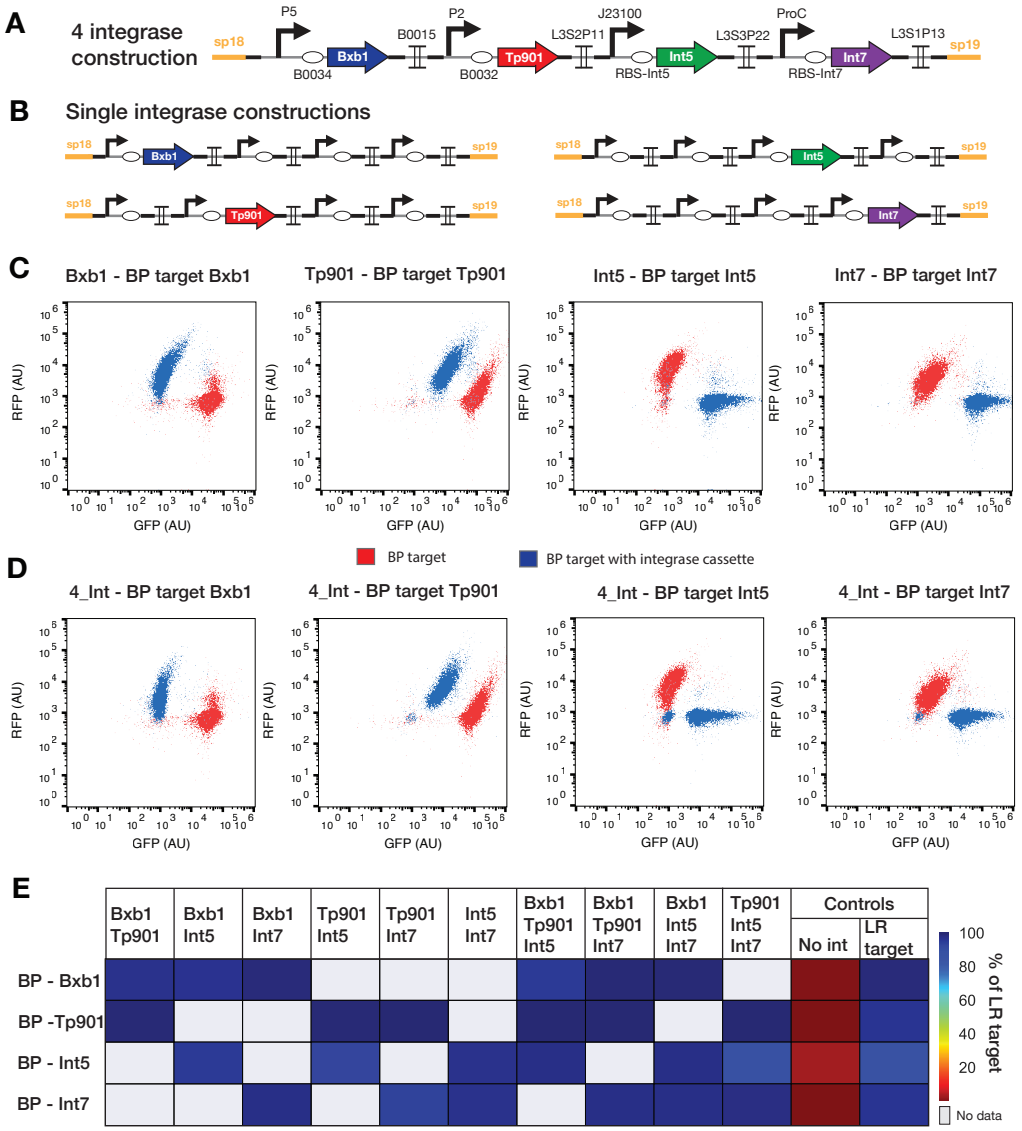

Figure S4: **Design and characterization of 16 constitutive integrase expression cassettes.** (A) The 4-integrase cassette is composed of the 4 integrase genes, a different ribosome binding site and promoter for each integrase, terminators to insulate each gene expression cassette and spacers to facilitate gibson assembly cloning. (B) The four single-integrase cassette. (C) Characterization of the four single-integrase cassette and (D) of the four-integrase cassette. Each single-integrase cassette was transformed with its BP target and the four-integrase cassette with each BP target, and after overnight culture, GFP and RFP fluorescence intensities were measured via flow-cytometer. The graphs correspond to density plots of the bacteria population with in x axis GFP fluorescence intensity in A.U. and in y axis RFP fluorescence intensity in A.U. The dots in blue correspond to the BP target with the corresponding integrase cassette and the dot in red correspond to the BP target alone as negative control of the switch. (E) Characterization of the two- and three-integrase cassettes. Each cassette was transformed with BP targets corresponding to the integrase it mediates expression, and after overnight, GFP and RFP fluorescence intensities were measured via flow-cytometer. For each target, on the GFP vs RFP density plot, a gate was defined on the switched population based on the LR target. The percentage of switched population is represented in the heatmap, data represented correspond to the mean of 3 replicates in one experiment. Each square corresponds to one BP target (labeled in y axis) and one integrase cassette (integrase corresponded labeled in x axis). The grey squares correspond to conditions for which no experiment was performed as the integrase corresponding to the BP target is not present in the integrase cassette.

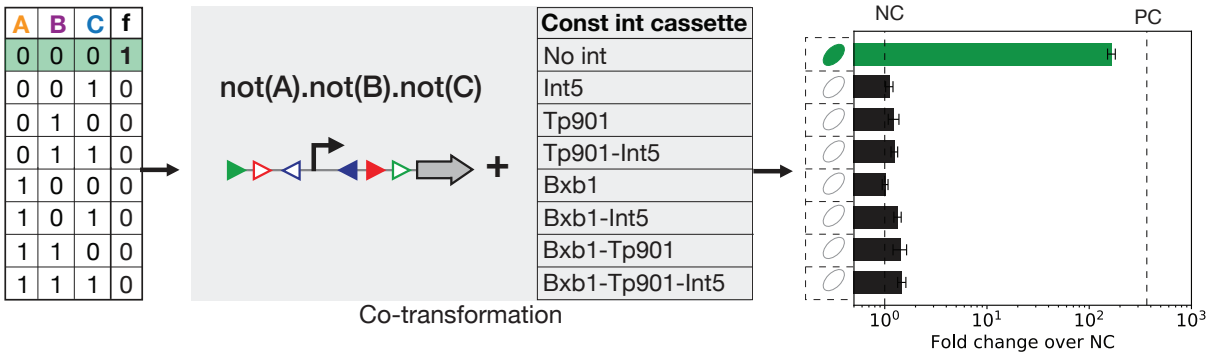

Figure S5: **Schematics of the workflow used to characterize recombinase logic devices.** Logic devices are characterized by co-transformation with constitutive integrase cassettes, one co-transformation corresponding to a specific input state (state of the truth table).

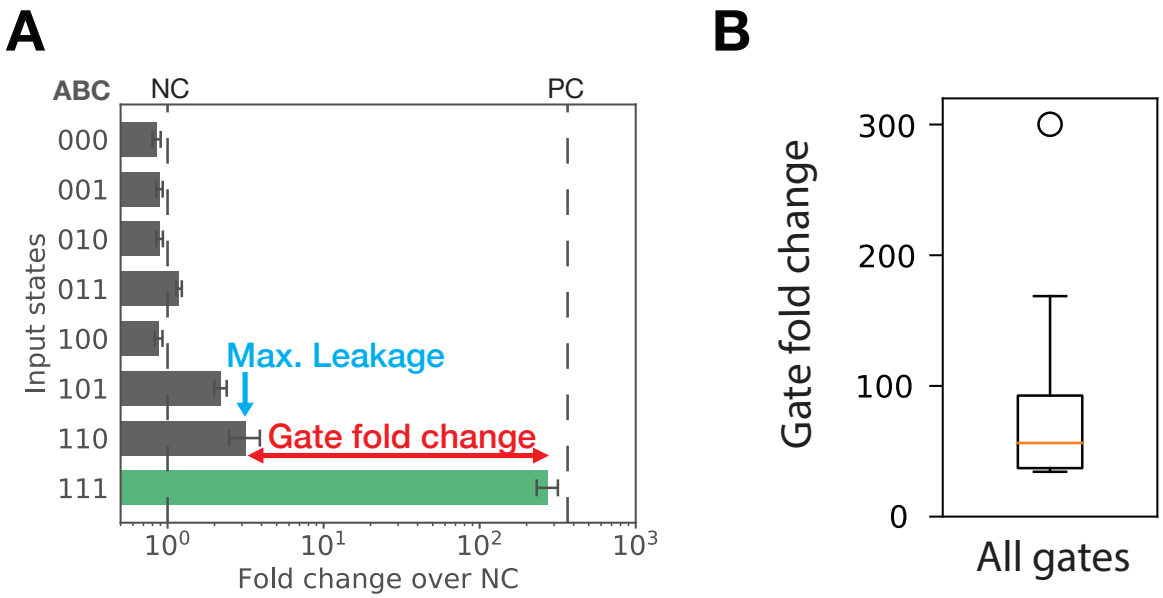

Figure S6: **Determination of the recombinase logic devices characteristics.** (A) Recombinase logic devices are characterized by a gate fold change and a maximum leakage. The gate fold change corresponds to the fold change between the ON state and the maximum OFF state, equivalent therefore to a minimum fold change. The maximum leakage corresponds to the fold change of the maximum OFF state. (B) Distribution of all 2 to 4-input gate fold changes.

# Logic device	# Gate fold change	# Maximum leakage
A.B	58	1.9
not(A).B	300	1.8
not(A).not(B)	169	1
A.B.C	86	3.2
not(A).B.C	42	11
not(A).not(B).C	34	3.2
not(A).not(B).not(C)	112	1.5
A.B.C.D	37	4.8
not(A).B.C.D	55	11
not(A).not(B).C.D	36	1.9
not(A).not(B).not(C).D	60	1.2
not(A).not(B).not(C).not(D)	34	4.5
not(A).B.C P6	15	3.2
not(A).B.not(C).not(D) P6	28	1.9

Table 1: **Recombinase device characteristics** The gate fold change corresponds to the fold change between the ON state and the maximum OFF state, equivalent therefore to a minimum fold change. The maximum leakage corresponds to the fold change of the maximum OFF state.

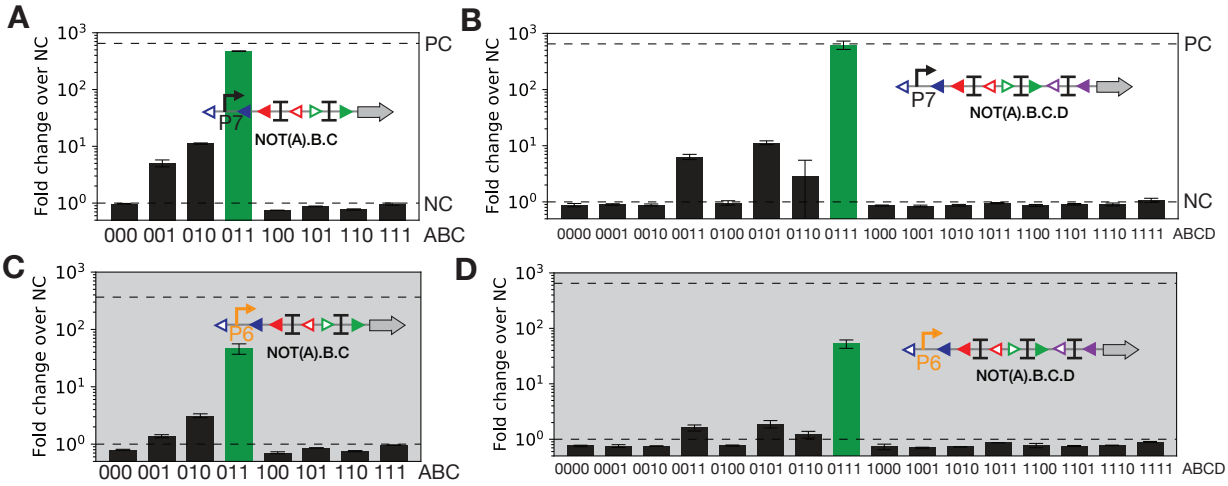

Figure S7: **Recombinase device tuning through change in transcription input signal.** We tuned the 2 devices with the highest background level by changing the promoter from P7 to P6. The characterization of the original devices not(A).B.C and not(A).B.C.D with the P7 promoter are represented in (A) and (B) respectively. (C) (D) Characterization of the devices with a weaker transcription input signal (P6 instead of P7).

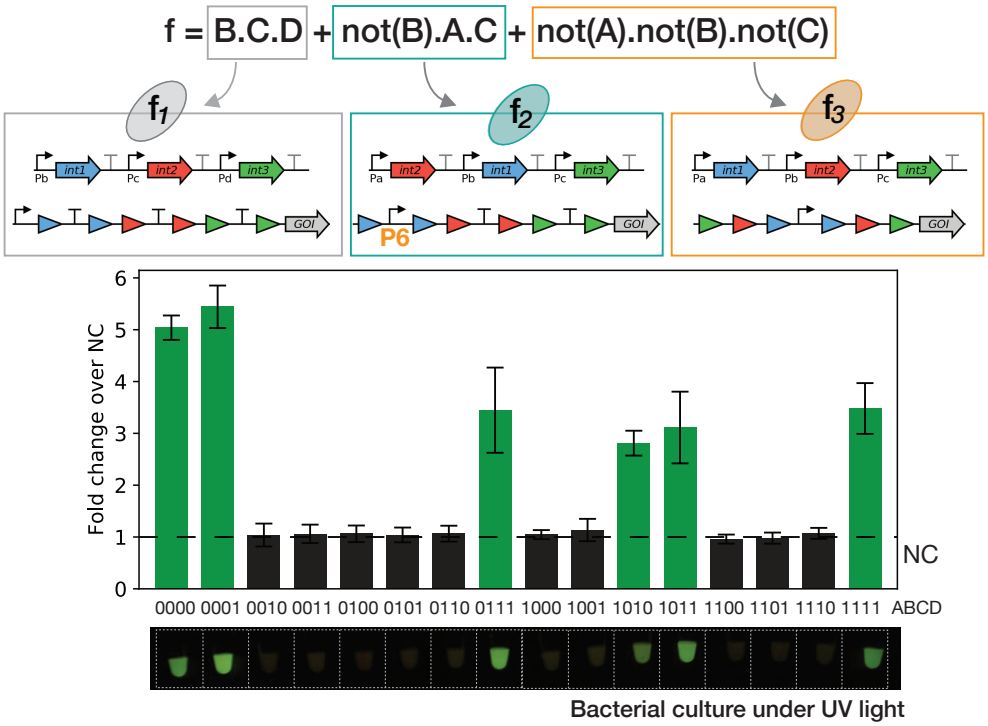

Figure S8: **A 4-input multicellular logic system using a device tuned by changing the transcription input signal.** Characterization of a multicellular logic system for the implementation of the logic function in Figure 3.C (f=B.C.D+not(A).A.C+not(A).not(B).not(C)) using the not(A).B.C logic device with P6 promoter. To prototype this logic system for each input state, we mixed the two strains containing the recombinase logic device and different constitutive integrase cassette corresponding to the different input states. After overnight growth, we measured the bulk fluorescence intensity of the whole-population using a plate reader. Bar graphs corresponds to the fold change in GFP median fluorescence intensity over the negative control. Data are from two experiments performed in different days with three replicates per experiment. Error bars: +/-SD. The photograph correspond to three co-culture replicates for each state centrifuged together, resuspended in 20 µL and observed under a UV light.

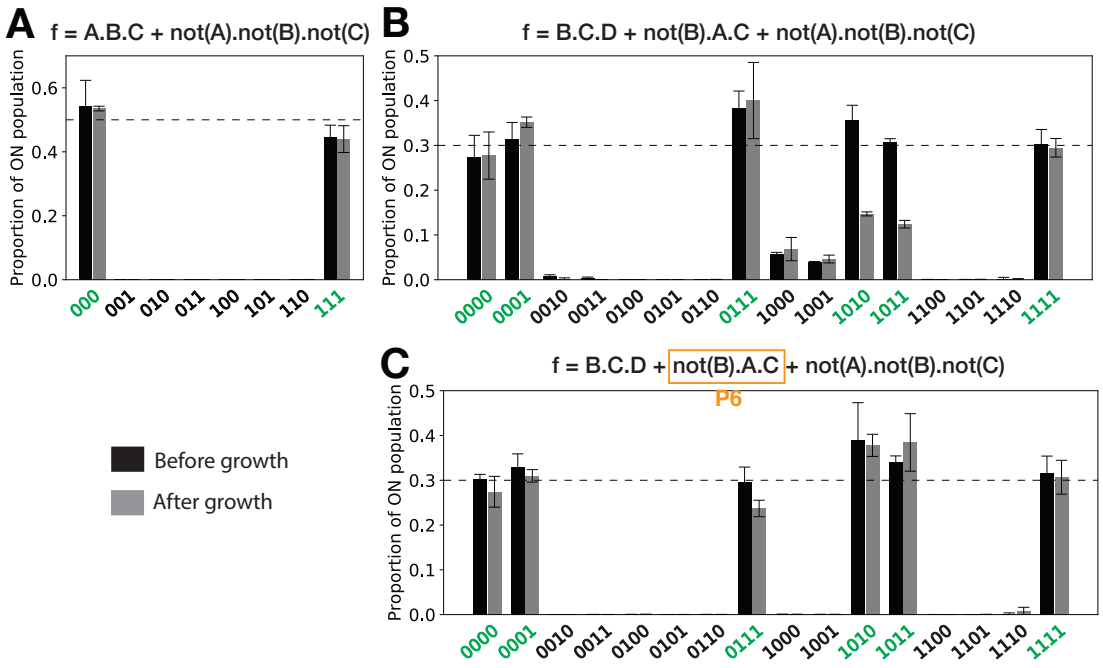

Figure S9: **Measurement of the proportions between the different strains of a multicellular system at different time points.** Proportion of ON cells in the total co-culture for each cell. Before (in black) and after overnight growth (in grey), single-cell fluorescence measurement of the co-culture is performed using flow-cytometer. Then, the proportion of cells expressing GFP is defined and plotted. X-axis correspond to the input state simulated by the analysed co-culture. Represented proportions are the mean of 2 experiments and the error bars correspond to the standard deviation between the two experiments.